

AD-A227 561

FTD-ID(RS)T-0579-90

FOREIGN TECHNOLOGY DIVISION



THE FABRICATION AND CHARACTERISTICS OF $\text{YBa}_2\text{Cu}_3\text{O}_{7-x}/\text{W}$ and $\text{Y}_2\text{O}_3/\text{W}$
FIELD EMITTERS

by

Xiang-Qi Jiang, Xi-Liang Yang, Hui Xu



DTIC
ELECTE
OCT 19 1990
S B D

Approved for public release;
Distribution unlimited.

HUMAN TRANSLATION

FTD-ID(RS)T-0579-90

24 September 1990

MICROFICHE NR: FTD-90-C-000906

THE FABRICATION AND CHARACTERISTICS OF $\text{YBa}_2\text{Cu}_3\text{O}_{7-x}/\text{W}$
and $\text{Y}_2\text{O}_3/\text{W}$ FIELD EMITTERS

By: Xiang-Qi Jiang, Xi-Liang Yang, Hui Xu

English pages: 10

Source: Dianzi Xuebao, Vol. 17, Nr. 6,
November 1989, pp. 101-104

Country of origin: China

Translated by: SCITRAN

F33657-84-D-0165

Requester: FTD/TTTRL/2Lt Leanne J. Henry

Approved for public release; Distribution unlimited. I

For

☒

☐

☐

d

Justification

By

Distribution/

Availability Codes

Dist

Avail and/or

Special

A-1

THIS TRANSLATION IS A RENDITION OF THE ORIGINAL FOREIGN TEXT WITHOUT ANY ANALYTICAL OR EDITORIAL COMMENT. STATEMENTS OR THEORIES ADVOCATED OR IMPLIED ARE THOSE OF THE SOURCE AND DO NOT NECESSARILY REFLECT THE POSITION OR OPINION OF THE FOREIGN TECHNOLOGY DIVISION

PREPARED BY:

TRANSLATION DIVISION
FOREIGN TECHNOLOGY DIVISION
WPAFB, OHIO

GRAPHICS DISCLAIMER

All figures, graphics, tables, equations, etc. merged into this translation were extracted from the best quality copy available.

The Fabrication and Characteristics of $\text{YBa}_2\text{Cu}_3\text{O}_{7-x}/\text{W}$ and $\text{Y}_2\text{O}_3/\text{W}$ Field Emitters

Jiang, Xiang-Qi; Yang, Xi-Liang; and Xu, Hui

(Modern Physics Institute, Fu-Dan University, Shanghai, China)

(Manuscript received in May, 1988, revised in November, 1988)

Abstract: The $\text{Y}_2\text{O}_3/\text{W}$ and $\text{YBa}_2\text{Cu}_3\text{O}_{7-x}/\text{W}$ field emitters have been fabricated and the corresponding field emission patterns have been obtained. For the same dimensions and parameters, the field emission current of $\text{Y}_2\text{O}_3/\text{W}$ is higher and more stable than that of W tip. By measuring field emission currents and voltages and plotting the data in accordance with the Fowler-Nordheim equation, the work function of $\text{YBa}_2\text{Cu}_3\text{O}_{7-x}/\text{W}$ was found to be 4.1eV at room temperature.

I. Introduction

Thermal Field Emission (TFE) can be applied to obtain high intensity brightness and, therefore, has been under scientific study in recent years.^[1] The choice of appropriate materials for the fabrication of the field emitter is an important topic in the study of thermal field emission. Rare earth metallic compound is a new area in the selection of the materials for the emitter. These compounds have the characteristics of high melting points, high ionic impact toughneses, toxicant resistances, high voltage tolerances, low work functions and the capability of operation under somewhat less perfect vacuum conditions. Among them, Y_2O_3 has been proved^[2,3] to be one of the best thermal field emitters. However, so far there has been very little report on its application in the field emission. In this paper, we will report the fabrication of the $\text{Y}_2\text{O}_3/\text{W}$ thermal field

emitter and the characterization of its field emission properties. This will serve as an introduction of the application of rare earth metallic oxides in the thermal field emission.

In 1987, a worldwide research heat of superconductors was triggered and an entire set of high-temperature oxide superconductors were fabricated. The electrical and magnetic properties, crystal structure and other related physical and chemical properties of $\text{YBa}_2\text{Cu}_3\text{O}_{7-x}/\text{W}$ superconductor were studied extensively. In this paper, the fabrication and testing of $\text{YBa}_2\text{Cu}_3\text{O}_{7-x}/\text{W}$ thermal field emitter are reported and the related thermal field emission characteristics data are given.

II. Fabrication of Thermal Field Emitters

In order to fabricate the $\text{YBa}_2\text{Cu}_3\text{O}_{7-x}/\text{W}$ and $\text{Y}_2\text{O}_3/\text{W}$ field emitters, the W needle tip should be fabricated first. The geometrical dimension, shape, surface cleanliness, and crystal structure of the tungsten needle tip have import effect on the emission characteristics of the two field emitters made from the tungsten needle tip. In this experiment, the electrolytic corrosion technique was used to fabricate the tungsten needle tip. The tip radius was on the order of 10^3\AA and the height was about $60\mu\text{m}$.

The tungsten needle tip was cleaned in the solution, baked dry, and heat treated in the ultra-high vacuum system with a purpose to clean up the surface of the needle tip and recrystallize the tungsten at the needle tip. The crystal at the needle tip grew and eventually a single crystal was formed so that the various typical field emission patterns of tungsten can be obtained.

The $\text{YBa}_2\text{Cu}_3\text{O}_{7-x}/\text{W}$ and $\text{Y}_2\text{O}_3/\text{W}$ emitters were fabricated by plating a small quantity of $\text{YBa}_2\text{Cu}_3\text{O}_{7-x}$ and Y_2O_3 powders on the surfaces of tungsten

needles which had the field emission patterns with (110) plane in the center. The fabrication process was followed by some adequate treatments.

The Y-Ba-Cu-O superconductor was fabricated according to the method introduced in reference [4].

III. Experiment and Results

The tungsten needle was placed in the vacuum chamber with anode plate installed. The tungsten anode was then pre-heated electrically in vacuo until the temperature of 1600C was reached (with a corresponding current of 2.5A in this experiment). If a negative high voltage were applied to the cathode and the zero electrical potential was connected to the anode, then the emission pattern of tungsten can be seen on the luminescence screen. Different voltages, temperatures, and residual gas environments will result in different emission patterns. If the voltage is 7.5kV (negative) and the instantaneous pre-heat current is 2.0A and the steady state heating current is 1.3A, then the field emission pattern and the corresponding crystallographic diagram are shown in figure 1 in which the two brightest lighted spots correspond to the emission of (130) and (010), and (310) and (100) crystal planes, the other lighted spots correspond to the emission of {111} and {122} families of crystal planes. The field current was 1.2 μ A. The tungsten emission current was very unstable; with pulse-like fluctuations and was decreasing with time.

After plating the tungsten needle with small quantity of Y₂O₃ powders, it was also necessary to conduct the heat treatment in vacuo. The temperature for this heat treatment was between 1600 and 1750C and the time was about 1 minute. The field emission pattern (after heat treatment) is shown in figure 2 where the lighted spots correspond to the emission of

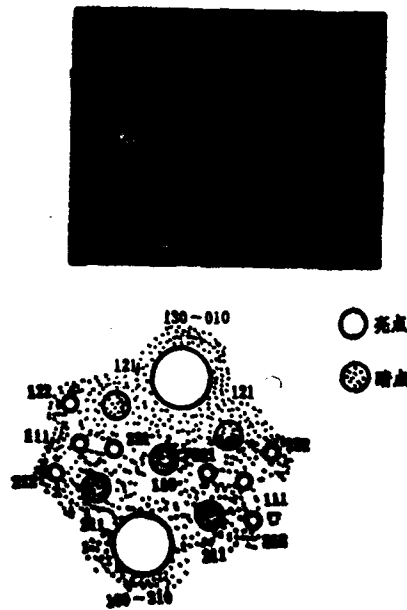


Figure 1: The tungsten field emission pattern and the corresponding crystallographic diagram ($V=7.5\text{kV}$, $i_m=2.0\text{A}$, $i_f=1.3\text{A}$).

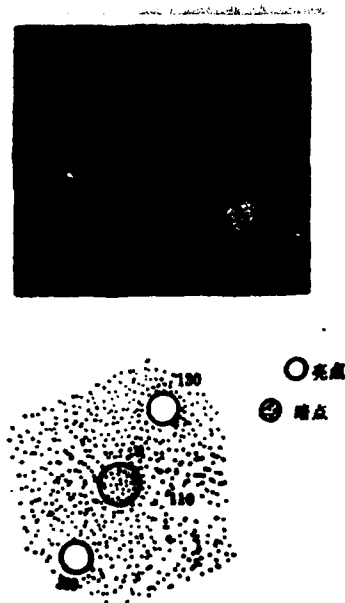


Figure 2: The field emission pattern of $\text{Y}_2\text{O}_3/\text{W}$ cathode and its corresponding crystallographic diagram ($V=3.0\text{kV}$, $i_f=1.2\text{A}$).

(130) and (310) planes. The voltage was 3kV and the heating current was 1.2A and the field current of Y_2O_3/W was $0.66\mu A$. Under the same parameters, the field current of tungsten anode was less than $10^{-8}A$. The change in Y_2O_3/W field current with time was measured under a vacuum of $4 \times 10^{-6}Pa$, a voltage of 4kV, and a heating current of 1.5A. The results are shown in figure 3. There is no pulse-like fluctuations in the current but the current increases slightly with time.

After the Y_2O_3/W field cathode was used for some time, its field current tended to decrease. It was necessary to heat treat the anode for a short time period in $10^{-6}Pa$ vacuum to resume its characteristics.

Figures 4 (a) and (c) show the scanning electron micrographes of a tungsten needle and its tip, whereas (b) and (d) are the corresponding micrographes after plating of $YBa_2Cu_3O_{7-x}$ powders. The treatment was carried out by heating in ultra-high vacuo or in small quantity of oxygen flow. During the treatment process, various patterns were seen on the luminescence screen and, finally, the field emission pattern shown in figure 5 was produced (with voltage of 6.5 - 9.0kV, heating current 2.0A and field emission current between 0.2 and $0.6\mu A$). When the vacuum is below $10^{-5}Pa$, the results are shown figure 6. The $YBa_2Cu_3O_{7-x}/W$ field anode follows the Fowler-Nordheim equation; namely, the relationship between $\log I/V^2$ and I/V is linear. The slope of this line and the needle diameter can be used to calculate the work function of the cathode and it was found to be 4.1eV.

IV. Discussions

After the treatment at 1600C, crystals with large dimensions will form at the tip of the tungsten needle. Since the tip radius is much smaller

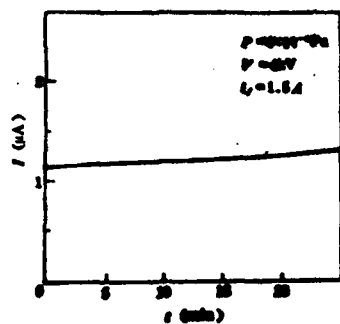


Figure 3: The time-variation of the emission current of $\text{Y}_2\text{O}_3/\text{W}$ cathode.

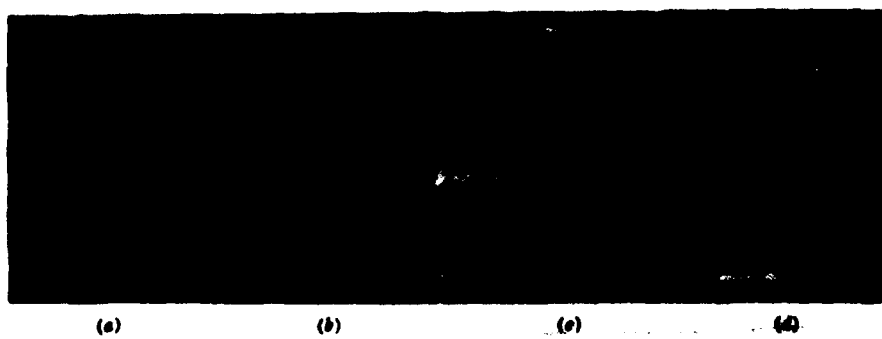


Figure 4: The micrographes of tungsten needle tip before ((a) and (c)) and after ((b) and (d)) plating of $\text{YBa}_2\text{Cu}_3\text{O}_{7-x}/\text{W}$ powder.

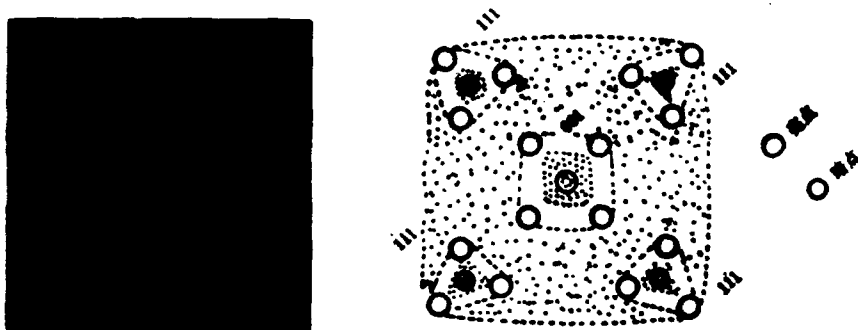


Figure 5: The field emission pattern (left) and its corresponding crystallographic diagram of YBa₂Cu₃O_{7-x}/W cathode.

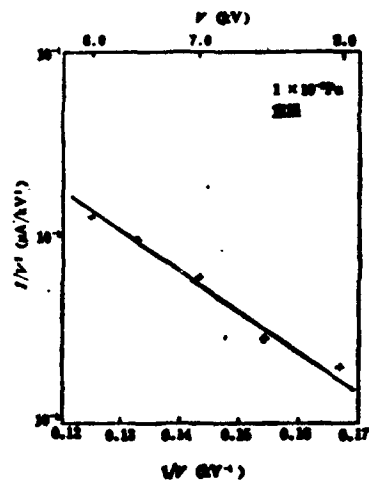


Figure 6: The relationship between $\log I/V^2$ and $1/V$ for YBa₂Cu₃O_{7-x}/W cathode at room temperature.

than the dimension of the crystals, the single crystal field emission patterns will be generated. Different crystal planes will have different work functions. Generally, the work functions of (310), (111) and (100) planes are small and bright spots in the emission patterns are associated with these planes, whereas the work functions of (110) and (211) planes are somewhat higher and dark spots are associated with these planes. [5]

However, under the conditions of thermal field emission, since the surface atoms will migrate and agglomerate towards certain crystal planes, the restructuring of these planes or formation of convex edges will be resulted. On the other hand, due to the diffusion of the dying agent in the tungsten needle and the evaporation from the surface, various surface phases will form at various temperatures on various planes. [6] Therefore, the brightnesses of the spots of the emission patterns are not singly determined by the work functions of the original crystal planes and different patterns will form at different temperatures and different field strengthes.

The atoms on the surface of the tungsten needle are different from the atoms in the body. The surface atoms have unsaturated hanging chains and very strong chain-forming forces. This will result in the adsorption of most foreign atoms on the surface. The adsorbed atoms on the various crystal planes of tungsten surface are adsorbed selectively and the work functions of various crystal planes are modified. The adsorption of Y_2O_3 on (310) and (130) planes results in the enhanced emission of electrons from the nearby crystal planes and the emission of electrons from other crystal planes was restricted. This is similar to the discovery described in reference [7] where the tungsten needle was immersed in the $Mg(NO_3)_2$ solution and then treated at high temperature in an oxygen environment to

obtain enhanced electron emission from (100) planes of the MgO/W (100) cathode. The explanation of this enhanced emission lies with the cooperation of the electrons from the adsorbed atoms and the electrons from the tungsten atoms of the substrate so that the emission electrons can be supplied continuously.

One of the important reasons for the instability of the tungsten field emission current was due to the adsorption and decomposition of the residual gas atoms on the surface of the tungsten needle. If a foreign atom is firmly attached to the surface of the tungsten needle and the unsaturated chain is made saturated, then the residual atoms can no longer be attached to the surface easily. Even if there is some adsorption, the effect on the field emission will still be insignificant. This is the reason why the field emission current of Y_2O_3/W is more stable than the tungsten field emission.

From the symmetry of the $YBa_2Cu_3O_{7-x}/W$ field emission patterns, it can be judged that the tip of the needle has the cubic crystal structure. However, most researches believed that there are three phases (A, B and C) of the Y-Ba-Cu-O material. The A and B phases have the simple orthogonal structures where the C phase has the body center cubic structure but with a much larger crystal constant than tungsten. [8,9] Hence, the reasons for the formation of the field emission patterns mentioned above is still unknown and further study is required.

This work was supported by Mr. Wei-On Luo and Mr. Guo-Tai Jung. The authors wish to express their sincere thanks to them.

REFERENCES

- [1] L. W. Swanson: J. Vac. Sci. Technol., Vol. 12, No. 6, p.1228, 1975

- [2] Li, Siao-Liaing: Electronic Scriptica, No. 1, p.48, 1965
- [3] Chen, Er-Gang: Instrument and Instrumentation Journal, No. 2, p.18, 1981
- [4] Luo, Wei-On et al.: Fu-Dan Scriptica (Natural Science Vol), Vol. 26, No. 3, p.253, 1987
- [5] E. W. Muller: J. A. P., Vol. 26, No. 6, p. 732, 1955
- [6] Chen, Jia-Ho and Chen, Chiang-Yen: Surface Analysis Technology, Electronic Industry Publishing Company, p.96, 1987
- [7] S. Hosoki et al.: Proc. 29th Internal Field Emission Congr., p. 1089, 1982
- [8] Hua, Jung-I et al.: Fu-Dan Scriptica (Natural Science Vol.), Vol. 26, No. 3, p. 241, 1987
- [9] T. Siegrist et al.: Proc. Rev. B, Vol. 35, No. 13, p. 7137, 1987

DISTRIBUTION LIST

DISTRIBUTION DIRECT TO RECIPIENT

<u>ORGANIZATION</u>	<u>MICROFICHE</u>
C509 BALLISTIC RES LAB	1
C510 R&T LABS/AVEADCOM	1
C513 ARRADCOM	1
C535 AVRADCOM/TSARCOM	1
C539 TRASANA	1
Q591 FSTC	4
Q619 MSIC REDSTONE	1
Q008 NTIC	1
E053 HQ USAF/INET	1
E404 AEBC/DOR	1
E408 AFWL	1
E410 AD/IND	1
F429 SD/IND	1
P005 DOE/ISA/DDI	1
P050 CIA/OCR/ADD/SD	2
AFTT/LDE	1
NOIC/OIC-9	1
CCV	1
MIA/PHS	1
LLVL/CODE L-309	1
NASA/NST-44	1
NSA/T513/TDL	2
ASD/FTD/TTIA	1
FSL	1